



ARTICLE

Impedance Response Alginate-Polyvinyl Alcohol Bio-Polymer Blend Electrolytes Doped with Ammonium Iodide

M. A. H. Nizam¹, A. F. Fuzlin^{1,2} and A. S. Samsudin^{1,2,*}

¹Ionic Materials Team, Faculty of Industrial Sciences & Technology, Universiti Malaysia Pahang Al-Sultan Abdullah, Kuantan, 26300, Pahang, Malaysia

²Centre for Advanced Intelligent Materials, Faculty of Industrial Sciences & Technology, Universiti Malaysia Pahang Al-Sultan Abdullah, Kuantan, 26300, Pahang, Malaysia

*Corresponding Author: A. S. Samsudin. Email: ahmadsalihin@ump.edu.my

Received: 01 October 2024 Accepted: 16 December 2024 Published: 27 March 2025

ABSTRACT

This work explores the dielectric and electrochemical properties of solid biopolymer blend electrolytes (SBEs) based on a combination of alginate and polyvinyl alcohol (PVA), doped with varying concentrations of ammonium iodide (NH₄I). The SBEs were synthesized using the solution casting method, and their ac conductivity exhibited an optimal value of $1.01 \times 10^{-5} \text{ S} \cdot \text{cm}^{-1}$ at 25 wt.% NH₄I. Detailed dielectric and modulus spectroscopy analyses revealed distinctive trends in relation to NH₄I concentration, suggesting complex dielectric relaxation behavior. The universal power law (UPL) analysis identified the Small Polaron Hopping (SPH) mechanism as the dominant conduction process in the optimal sample. These results demonstrate that NH₄I-doped alginate-PVA SBEs possess favorable electrochemical properties, positioning them as potential candidates for energy storage and ionic transport devices.

KEYWORDS

Impedance-frequency dependence; bio-polymer electrolytes; ac conductivity; SPH model

1 Introduction

Energy forms the material foundation of human life and social progress, and its storage is essential for efficient development and utilization [1]. However, the increasing reliance on conventional, non-renewable energy sources, particularly carbon-based fuels, has contributed to severe environmental degradation. The global energy crisis, coupled with escalating concerns over climate change, air pollution, and the depletion of natural resources, has prompted a shift toward sustainable and eco-friendly alternatives. This urgency drives researchers to explore renewable energy solutions that mitigate the harmful effects of traditional energy systems, such as global warming, energy insecurity, and public health risks.

Polymer electrolytes have emerged as promising materials for energy storage devices due to their diverse electrochemical properties [2]. Polymer electrolytes are a diverse group of materials



characterized by long polymer chains and relatively high concentrations of ions [3]. These materials have long been interesting due to their potential applications in various current and emerging technologies [4–7]. Among them, solid biopolymer electrolytes (SBEs), derived from renewable natural sources, have gained attention for their environmental benefits, high ionic conductivity, and improved electrode-electrolyte interface [8,9]. They primarily include polynucleotides, polypeptides, and polysaccharides [10]. Among them, polypeptides and polysaccharides are the most commonly used, including materials like gelatin, alginate, starch, agar, cellulose, and chitosan [11]. Unlike their liquid or gel-based counterparts, SBEs offer superior safety by eliminating leakage risks, making them suitable for batteries, fuel cells, and capacitors [12]. Therefore, SBEs can serve as electrolytes, efficiently transporting ions between the cathode and anode [13]. However, the crystalline nature of biopolymers such as polyvinyl alcohol (PVA) and chitosan often limits ionic mobility, reducing ionic conductivity [14]. To address this challenge, several strategies have been explored, such as incorporating ionic liquids [15], blending polymers [16], adding plasticizers [17], and integrating fillers [18].

In many fields, homopolymers or copolymers alone may not always meet all the requirements for practical use [19]. Thus, the blending method, which involves combining with other polymers, has become an alternative approach to modifying these materials' structural and electrical properties, thereby expanding their range of applications [20,21]. Research on the blending method has focused on intermolecular complexation as a key factor in enhancing amorphousness and conductivity [22]. It has shown significant potential in enhancing ionic conductivity by reducing activation energy and disrupting intermolecular forces, thus improving ion transport [23]. Polymer blends have gained greater commercial and technological significance compared to the production of homopolymers and copolymers as it enables the creation of new materials with tailored properties for specific applications at a lower cost [24]. Polyvinyl alcohol (PVA) is a notable candidate as a secondary polymer as it is a non-toxic, synthetic, semi-crystalline, biodegradable, cost-effective, and FDA-approved polymer [25]. It comprises a carbon chain backbone with hydroxyl groups attached to the carbon atoms of methane, which acts as a source of hydrogen bonding and assists in forming a polymer blend [26]. Studies on alginate-PVA biopolymer blends have demonstrated improved ionic conductivity compared to single polymer systems, with values reaching up to $7.52 \times 10^{-8} \text{ S} \cdot \text{cm}^{-1}$. Ionic dopants are another crucial factor in enhancing the segmental motion of polymer chains, thereby facilitating ion migration. Ammonium salts, in particular, are known for their low lattice energy, which promotes the release of free ions, increases ionic conductivity and are good proton donors to the polymer matrix [27]. Ammonium iodide (NH_4I), a combination of ammonium (NH_4^+) and iodide (I^-) ions, has shown superior performance in past studies [28]. For instance, PVA-based systems doped with NH_4I achieved higher ionic conductivities ($2.5 \times 10^{-3} \text{ S} \cdot \text{cm}^{-1}$) compared to NH_4Br ($5.7 \times 10^{-4} \text{ S} \cdot \text{cm}^{-1}$) and NH_4Cl ($1.0 \times 10^{-5} \text{ S} \cdot \text{cm}^{-1}$) [29], mainly due to the lower lattice energy of NH_4I [30].

In light of these findings, this study aims to investigate the dielectric properties of alginate-PVA biopolymer blend electrolytes doped with ammonium iodide to evaluate their potential for future electrochemical applications.

2 Experimental Sections

2.1 Materials

Alginate (Alg) (4000 molecular weight; Sigma-Aldrich, St Louis, MO, USA) was purchased from China and partially hydrolyzed PVA $\sim 85\%$ (7000 molecular weight; Sigma-Aldrich, St Louis, MO, USA) was purchased from EMD Milipore Corporation, Germany where it acts as polymer blend host. Ammonium iodide (NH_4I) (molecular weight: $144.94 \text{ g mol}^{-1}$; Sigma-Aldrich, St Louis, MO, USA) was purchased from the USA and acted as an ionic dopant salt.

2.2 Preparation of SBEs

A solution casting method was carried out to prepare the solid biopolymer blend (SBE) system-based Alg-PVA doped with NH_4I . A homogenous solution was obtained by dissolving alginate and PVA in distilled water and stirring the mixture continuously until it was completely dissolved. Then, NH_4I was added to the solution in a range of c_0 , from 5 to 40 weight percentage (wt.%). The solutions were placed in petri dishes and dried in the oven at 60°C for 8 h. The petri dishes were kept in a desiccator to ensure that no solvent remained in the sample.

2.3 Characterization of BBEs

2.3.1 AC Conductivity Study

The ionic conductivity of the prepared SBEs sample was evaluated using a HIOKI 3532-50 LCR Hi-TESTER, purchased from HIOKI SINGAPORE PTE. LTD., Vertex, Singapore, over a frequency range of 50 Hz to 1 MHz. The SBE film was positioned between two stainless steel current collectors and tested within a temperature range of 303 to 343 K. and its thickness was determined using a digital thickness gauge (DML3032, purchased from RDM Test Equipment Ltd., UK). The ionic conductivity of the alginate-PVA- NH_4I film-based SBEs system was calculated using the equation provided (Eq. (1)):

$$\sigma = \frac{d}{R_b A} \quad (1)$$

where d is the thickness of the electrolytes, A is the contact area (cm^2), and R_b is the bulk resistance of the SBEs system obtained from the Cole-Cole plot.

2.3.2 Dielectric Study

The dielectric constant, ϵ_r , and loss, ϵ_i for the SBE system were defined by Eqs. (2) and (3):

$$\epsilon_r = \frac{Z_i}{\omega C_0 (Z_r^2 + Z_i^2)} \quad (2)$$

$$\epsilon_i = \frac{Z_r}{\omega C_0 (Z_r^2 + Z_i^2)} \quad (3)$$

Z_r and Z_i represent the real and imaginary components of the complex impedance, respectively, and C_0 is the vacuum capacitance, defined as $C_0 = \epsilon_0 A / D$. Here, d denotes the thickness of the polymer electrolyte, f is the frequency in Hz, ω is the angular frequency ($\omega = 2\pi f$) which corresponds to the minimum in the imaginary impedance, and ϵ_0 is the permittivity of free space ($8.85 \times 10^{-14} \text{ F cm}^{-1}$). Meanwhile, A represents the contact area between the electrolyte and the electrode.

The real modulus (M_r) and imaginary modulus (M_i) were computed using the following equations (Eqs. (4) and (5)):

$$M_r = \frac{\epsilon_r}{(\epsilon_r^2 + \epsilon_i^2)} \quad (4)$$

$$M_i = \frac{\epsilon_i}{(\epsilon_r^2 + \epsilon_i^2)} \quad (5)$$

2.3.3 Universal Power Conduction Mechanism

The ac conductivity was obtained following the relation [31] (Eq. (6)):

$$\sigma_\omega = A\omega^s + \sigma_{dc} \quad (6)$$

where σ_ω is the total conductivity, A is temperature dependent parameter, s is the power law exponent and σ_{ac} is the frequency-independent dc conductivity. The ac conductivity, σ_{ac} is presented by $A\omega^s$, hence (Eq. (7)):

$$\sigma_\omega = \sigma_{ac} + \sigma_{dc} \quad (7)$$

The σ_{ac} can be solved using the following (Eq. (8)):

$$\sigma_{ac} = \varepsilon_0 \varepsilon_i \omega \quad (8)$$

where $\varepsilon_r \tan \delta = \varepsilon_i$. By substituting $\sigma_{ac} = A\omega^s$ into Eq. (5), the value of s can be evaluated from the following relationship (Eq. (9)):

$$\sigma_{ac} = \varepsilon_0 \varepsilon_i \omega \quad (9)$$

The exponent s value is retrieved from the slope of the plot $\ln \varepsilon_i$ vs. $\ln \omega$.

3 Results and Discussion

3.1 AC Conductivity Study

Fig. 1 illustrates the frequency-dependent conductivity for alginate-PVA bio-polymer blend electrolytes doped with different compositions of ammonium iodide (NH_4I). The results indicate that the incorporation of NH_4I significantly enhances the ionic conductivity of the SBEs. As expected, the conductance spectra can be categorized into three distinct regions: the low-frequency dispersion region, the medium-frequency plateau, and the high-frequency dispersion region [32]. In the low-frequency region, a noticeable increase in conductivity with rising frequency is observed, which is characteristic of electrode polarization effects. This phenomenon can be attributed to space charge polarization occurring at the electrode-electrolyte interface, where the accumulation of charges increases conductivity as frequency increases [33]. At this stage, ionic motion is hindered by polarization, but higher frequencies alleviate the space charge effects, allowing ions to move more freely.

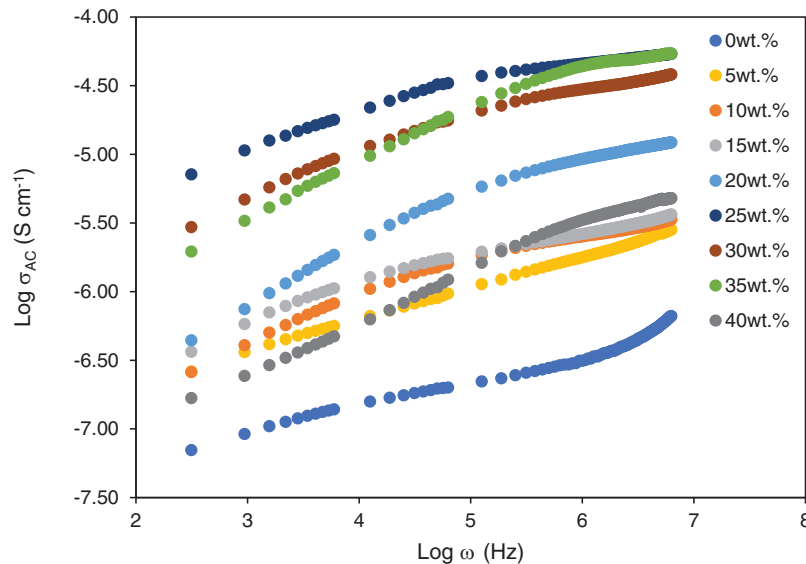


Figure 1: Frequency Dependence Conductivity for the samples at the different compositions of NH_4I

The frequency-independent plateau in the intermediate region represents the bulk conductivity of the system, which is a critical parameter for evaluating the efficiency of ion transport in the electrolyte

matrix [34]. The flatness of the conductivity in this region suggests that ion hopping between localized sites is occurring, and the contribution from mobile charge carriers within the biopolymer matrix dominates the overall conductivity. At higher frequencies, another increase in conductivity is observed, corresponding to the high-frequency dispersion region. This region is associated with bulk relaxation processes, where the coulombic interactions between charge carriers and the disordered polymer matrix become prominent [35]. The observed non-linear behaviour in this region indicates non-Debye type relaxation, which suggests that the system does not follow a simple dielectric relaxation model due to the structural heterogeneity within the electrolyte matrix. This is a common feature in complex polymer systems, where the interaction between charge carriers and the biopolymer chains is not uniform.

The highest ionic conductivity is achieved for the sample containing 25 wt.% NH_4I , with a value of $1.01 \times 10^{-5} \text{ S} \cdot \text{cm}^{-1}$. This optimum conductivity is attributed to the sufficient concentration of NH_4^+I^- , which enhances ion mobility by increasing the free volume in the polymer matrix and facilitating efficient ion transport. However, further increases in NH_4I concentration beyond 25 wt.% lead to a decline in conductivity. This decline can be explained by the formation of ion aggregates, causing the ion to be overcrowded and eventually restricts ion movement and limits the segmental motion of the polymer chain, leading to a reduction in ionic conductivity [36]. The excess ions form clusters, reducing the effective ionic mobility and increasing the overall ionic resistance of the system. The results demonstrate that while doping with NH_4I improves the ionic conductivity of the alginate-PVA blend, there is an optimal doping level beyond which the system becomes less efficient due to ion aggregation. This highlights the importance of finding the right balance between ionic dopants and polymer matrix composition to optimize electrochemical performance for potential applications in solid-state batteries and other energy storage devices.

Fig. 2 presents the plot of ac conductivity ($\log \sigma_{ac}$) as a function of frequency ($\log \omega$) for the sample containing 25 wt.% NH_4I at various temperatures. A clear shift in the conductivity profile is observed as the temperature increases. Specifically, the frequency at which dispersion becomes prominent shifts to the higher frequency region, and the conductivity dispersion region narrows with increasing temperature [37]. This behaviour can be attributed to the thermally activated nature of ionic conduction in the biopolymer blend. At lower temperatures, ionic movement is more restricted due to the reduced segmental motion of the polymer chains, resulting in lower conductivity values. However, as the temperature rises, the enhanced thermal energy facilitates greater polymer segmental mobility, allowing ions to move more freely through the electrolyte matrix. This increases ionic conductivity, as reflected in the upward shift in the $\log \sigma_{ac}$ values.

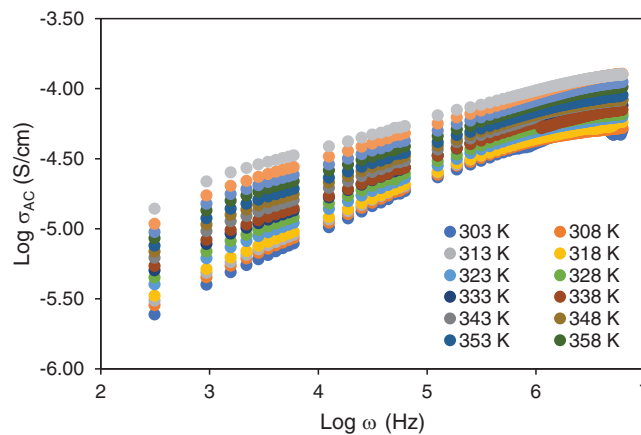


Figure 2: Frequency dependence conductivity for sample 25wt.% of NH_4I at different temperature

The observed increase in conductivity with temperature follows the trend described by Jonscher's universal power law. According to this model, the ac conductivity (σ_{ac}) consists of a frequency-independent component, corresponding to the dc conductivity (σ_{dc}), and a frequency-dependent component, which accounts for the hopping of ions between localized sites in the polymer matrix. The overall increase in conductivity with temperature is consistent with the thermally activated hopping mechanism, where ions gain sufficient energy to overcome potential barriers, thereby enhancing conduction.

3.2 Frequency-Immittance Analysis

Fig. 3a,b illustrates the variation in dielectric constant (ϵ_r) and dielectric loss (ϵ_i) as a function of NH₄I composition in the alginate-PVA bio-polymer blend electrolytes, measured at different frequencies. The dielectric constant (ϵ_r) represents the material's ability to store electrical energy, while the dielectric loss (ϵ_i) indicates the energy dissipated as heat in the system. The value of ϵ_i has increased sharply at low frequencies due to enhancement in the mobility of charge carriers. It can be related to the free charge motion within the electrolytes [38]. A trend that is typically associated with electrode polarization and space charge accumulation. This behaviour is driven by the polarization effect, where mobile ions within the electrolyte respond to the applied electric field, resulting in charge build-up at the electrode-electrolyte interface. The sharp rise in ϵ_i at low frequencies further confirms the presence of electrode polarization, suggesting a strong non-Debye relaxation behaviour. This is consistent with materials where charge carriers are not uniformly distributed and different relaxation times exist within the system.

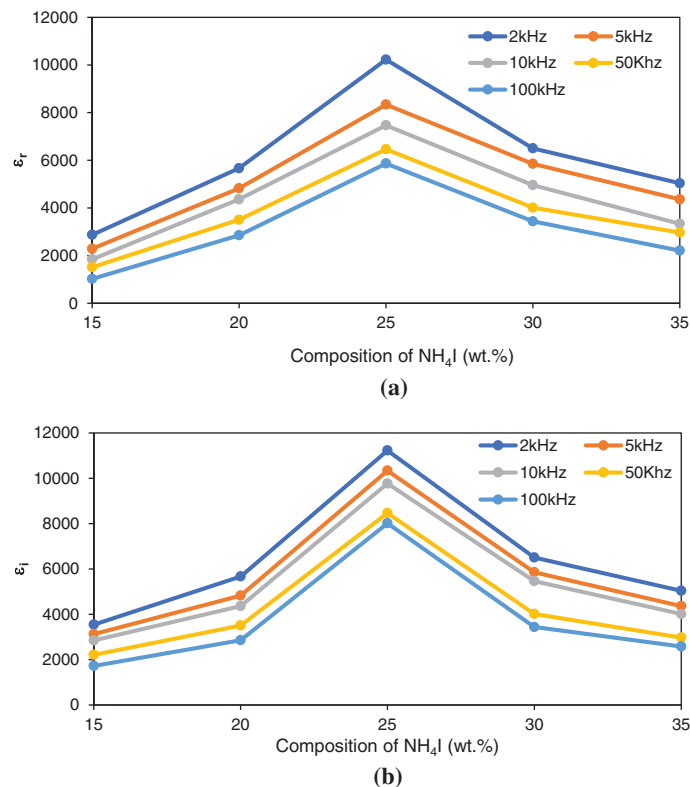


Figure 3: Dielectric (a) Constant and (b) Loss of SBEs system at ambient temperature

As the frequency increases, the values of ε_r and ε_i decrease. At higher frequencies, the rapid oscillation of the applied electric field prevents ions from following the field changes, leading to reduced polarization. Consequently, the space charge polarization effect is minimized, and there is less charge accumulation at the interface. This polarization decrease at high frequencies results in the reduced dielectric constant and dielectric loss observed in the plots [9]. The decline in ε_r and ε_i with increasing frequency indicates that ionic motion becomes less significant at high frequencies, where the periodic reversal of the field outpaces the mobility of the charge carriers. The peak in dielectric properties was observed at the 25 wt.% NH_4I composition in both ε_r and ε_i curves suggests an optimal concentration for ion transport and polarization. Previous research where alginate was doped with ammonium bromide (NH_4Br) also shows that the value declined once it reached optimal concentration at 20 wt.% [39]. Beyond this concentration, the decline in dielectric properties could be attributed to the formation of ion clusters, which reduce the number of free charge carriers and limit ion mobility. This supports the earlier observation from the ac conductivity analysis, where the 25 wt.% NH_4I sample exhibited the highest conductivity.

The results indicate that the dielectric properties of NH_4I -doped alginate-PVA biopolymer electrolytes are highly dependent on composition and frequency. At optimal NH_4I content and lower frequencies, the materials exhibit significant dielectric polarization, which benefits applications requiring high energy storage capacity. However, the reduction in polarization and charge accumulation at higher frequencies suggests that the material could also effectively minimise energy loss in high-frequency applications.

Fig. 4a,b shows real modulus, M_r , and imaginary modulus, M_i for the SBEs system. Both M_r and M_i show a plateau or approaches to zero at lower frequency and start to increase at higher frequency due to electrode polarization. At low frequency, the results almost approaching zero for all compositions associated with the high capacitance causes by the electrode polarization [40]. A long tail observed at low frequencies shows that a large capacitance may be attributed to electrode polarization effects encountered during impedance measurements, which further confirms the non-Debye behavior in the present sample [41]. For the 25 wt.% sample, both show low curve due to high dissociation of NH_4I , which lead to an increase in ionic conductivity of the present samples. Meanwhile, the curves at higher frequencies may result from bulk effects, with a decrease in curve height due to the ionic dopant, suggesting multiple relaxation mechanisms [42]. As frequency increases, the modulus component rises due to bulk polarization, which can be divided into two factors which are the electron transfer and avalanche transit-time [43]. The bulk effects can be seen in the current system due to electron transfer between the host polymer and the dopant system [44]. The presence of peak in imaginary part of the spectra, is believed due to capacitance behavior and segmental movement, are coupled and build up a peak in the modulus spectra [45]. Meanwhile, the disappearance of the peak for other samples is due to frequency limitation [44].

At higher frequencies, the increasing trend in M_r and M_i is indicative of bulk polarization effects. These effects arise from the limited movement of ions at higher frequencies due to their inability to follow the rapidly changing external field. The phenomenon can be further explained by electron transfer and avalanche transit-time mechanisms. In the current system, electron transfer between the host polymer and the dopant (NH_4I) contributes to the observed bulk effects, as the dopant enhances the overall conductivity by facilitating ion transport through the polymer matrix [44].

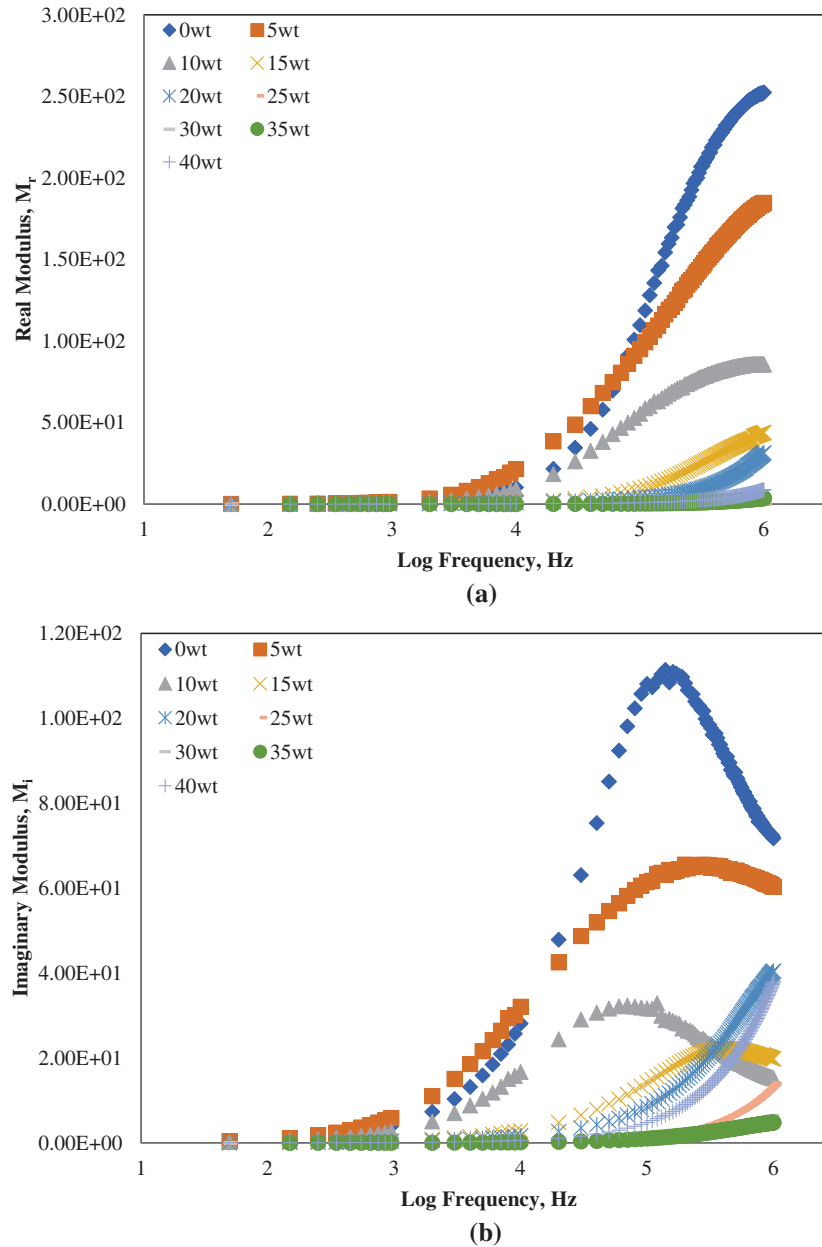


Figure 4: Frequency dependence of (a) Real modulus and (b) Imaginary modulus of the system at ambient temperature

3.3 Universal Power Law Mechanism

Fig. 5 depicts the plot of for the sample with the highest ionic conductivity (25 wt.% NH_4I) at elevated temperatures. The frequency range studied, $12 < \ln \omega < 16$, was selected due to the minimal effect of space charge polarization at higher frequencies [2]. In this range, the slope of the plot was calculated, corresponding to the value of the exponent s . This exponent is a critical factor in determining the ionic conduction mechanism, as it correlates with the theoretical hopping mechanism that involves the active coordination sites within the polymer matrix. Understanding the value of s provides insight into the dominant conduction mechanism at play within the system. Generally,

four distinct conduction mechanisms can be identified based on the value of the exponent s . These mechanisms include Quantum-Mechanical Tunneling (QMT), where charge carriers traverse potential barriers via quantum tunneling. Correlated Barrier Hopping (CBH) involves charge carriers hopping over energy barriers correlated with the material's energy landscape. Another prominent mechanism is Small Polaron Hopping (SPH), where localized charge carriers hop between adjacent sites within the material. Lastly, the Overlapping-Large Polaron Tunneling (OLPT) [46] mechanism suggests that large polarons tunnel through barriers, characterized by overlapping wave functions.

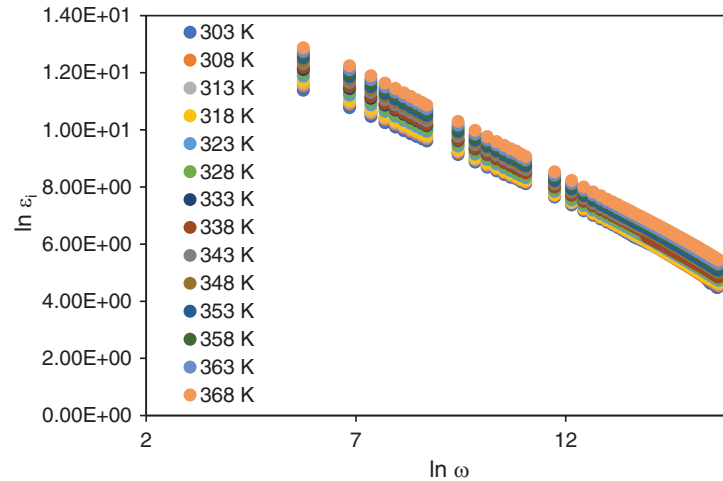


Figure 5: Plot of $\ln \epsilon_i$ vs. $\ln \omega$ for the highest ionic conductivity, Alg-PVA-NH₄I (25 wt.%)

The determination of the appropriate conduction mechanism depends on how the exponent s varies with temperature. Previous studies have investigated the temperature dependence of s to explain conduction mechanisms in disordered materials such as amorphous semiconductors [46]. In this study, the relationship between s and temperature offers important insights into the ion hopping behaviour within the biopolymer matrix and helps elucidate the role of the NH₄I dopant in enhancing ionic conductivity in the system.

Fig. 6 presents the variation of the frequency exponent s with temperature for the sample exhibiting the highest ionic conductivity (25 wt.% NH₄I). The value of s is a key parameter in determining the conduction mechanism in disordered materials, which is often temperature-dependent. As shown in the plot, the value of s increases as the temperature rises, following a linear relationship, as represented by the equation $s = 0.0012T + 0.3636$. This temperature dependence of s suggests that thermally activated processes dominate ion transport in the present system. The increase in s with temperature indicates that at higher temperatures, ions gain sufficient energy to overcome potential barriers, thus facilitating more effective conduction through the polymer matrix. This observation aligns with the Small Polaron Hopping (SPH) model, which is frequently used to describe ion conduction in disordered materials, particularly at higher temperatures [47]. According to small-polaron hopping theory, two types of hopping are distinguished: “adiabatic” hopping, where ions remain relaxed within the potential well of the lattice distortion throughout the process, and “anti-adiabatic” hopping, where ions jump out of the potential well, allowing the lattice to equilibrate to a new position. In the latter, pathways created by biopolymer-salt complexes help attract electrons from the biopolymer [48].

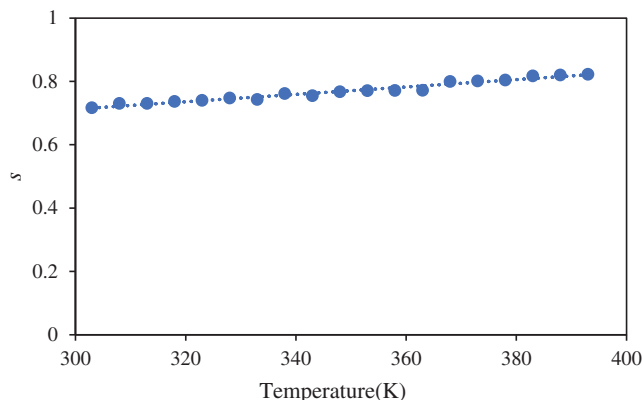


Figure 6: Plot s vs. T for 25 wt.% of NH_4I

In the SPH model, conduction occurs via the hopping of localized charge carriers (such as small polarons) between neighbouring sites in the material. At elevated temperatures, the thermal energy available to the ions allows them to hop more easily between these localized sites, increasing the exponent s . This mechanism is consistent with the observed behavior in your system, where the rise in s with temperature reflects the enhanced mobility of ions facilitated by thermally activated hopping. The gradual increase in s also suggests that the interactions between charge carriers and the polymer matrix primarily govern ion movement. As the temperature increases, the polymer chains become more flexible, reducing the energy barriers for ion hopping and thereby promoting more efficient ionic transport. This supports the notion that the conduction mechanism in the NH_4I -doped alginate-PVA biopolymer electrolytes is strongly influenced by both the polymer segmental motion and the hopping of charge carriers.

4 Conclusion

Conducting biopolymers, alginate-PVA doped with NH_4I biopolymer electrolytes, were successfully prepared via a solution casting technique.

- In this study, the impedance properties of NH_4I -doped alginate-PVA biopolymer blend electrolytes were investigated, revealing a significant enhancement in ionic conductivity, with the highest value of $1.01 \times 10^{-5} \text{ S} \cdot \text{cm}^{-1}$ observed at 25 wt.% NH_4I .
- Dielectric analysis showed that electrode polarization dominated at low frequencies, while bulk material properties became more prominent at higher frequencies. These measurements demonstrated non-Debye relaxation behaviour, indicating that the conduction mechanism in the SBEs does not follow a simple dielectric relaxation model, likely due to the disordered nature of the polymer blend and the interactions between mobile ions and the polymer chains.
- The modulus and frequency exponent s analyses indicated that the conduction mechanism follows the Small Polaron Hopping (SPH) model, confirming that ion transport is thermally activated and influenced by the disordered polymer matrix. These findings demonstrate that NH_4I -doped alginate-PVA biopolymer electrolytes hold great promise for applications in electrochemical devices, particularly in energy storage systems.

Acknowledgement: The authors would like to thank the Faculty of Industrial Sciences and Technology, UMPSA and Ionic Materials Team for the laboratory facilities.

Funding Statement: University Malaysia Pahang Al-Sultan Abdullah (UMPSA) under the UMPSA Distinguish Grant (RDU233001) and Ministry of Higher Education Malaysia (MOHE) under the FRGS fund (FRGS/1/2023/STG05/UMP/02/2).

Author Contributions: Draft preparation, Methodology, Investigation, Writing and Editing: M. A. H. Nizam; Data Validation, Methodology, Writing, and Editing, Co-Supervision: A. F. Fuzlin; Reviewing, Validation, Conceptualization, Funding, Supervision, and Visualization: A. S. Samsudin. All authors reviewed the results and approved the final version of the manuscript.

Availability of Data and Materials: The data that support the findings of this study are available from the corresponding author upon reasonable request.

Ethics Approval: Not applicable.

Conflicts of Interest: The authors declare no conflicts of interest to report regarding the present study.

References

1. Huo S, Sheng L, Xue W, Wang L, Xu H, Zhang H, et al. Challenges of polymer electrolyte with wide electrochemical window for high energy solid-state lithium batteries. *InfoMat*. 2023;5(3):e12394. doi:10.1002/inf2.v5.3.
2. Abdulkadir BA, Ojur Dennis J, Al-Hadeethi Y, Shukur M, Mkawi EM, Al-Harbi N, et al. Optimization of the electrochemical performance of a composite polymer electrolyte based on PVA-K₂CO₃-SiO₂ composite. *Polymers*. 2020;13(1):92.
3. Bocharova V, Sokolov AP. Perspectives for polymer electrolytes: a view from fundamentals of ionic conductivity. *Macromolecules*. 2020;53(11):4141–57. doi:10.1021/acs.macromol.9b02742.
4. Hallinan DT, Balsara NP. Polymer electrolytes. *Annu Rev Mater Res*. 2013;43:503–25. doi:10.1146/matsci.2013.43.issue-1.
5. Hu L, Zhang Q, Li X, Serpe MJ. Stimuli-responsive polymers for sensing and actuation. *Mat Horizons*. 2019;6(9):1774–93. doi:10.1039/C9MH00490D.
6. Le NL, Nunes SP. Materials and membrane technologies for water and energy sustainability. *Sustain Mat Technol*. 2016;7:1–28. doi:10.1016/j.susmat.2016.02.001.
7. Leones R, Sabadini RC, Sentanin FC, Esperança JMSS, Pawlicka A, Silva MM. Polymer electrolytes for electrochromic devices through solvent casting and sol-gel routes. *Solar Energy Mat Solar Cells*. 2017;169:98–106. doi:10.1016/j.solmat.2017.04.047.
8. Wang N, Zhang XX, Liu HH, He BQ. 1-Allyl-3-methylimidazolium chloride plasticized-corn starch as solid biopolymer electrolytes. *Carbohyd Polym*. 2009;76(3):482–4. doi:10.1016/j.carbpol.2008.11.005.
9. Rani MSA, Mohamed NS, Isa MIN. Investigation of the ionic conduction mechanism in carboxymethyl cellulose/chitosan biopolymer blend electrolyte impregnated with ammonium nitrate. *Int J Polym Anal Character*. 2015;20(6):491–503. doi:10.1080/1023666X.2015.1050803.
10. Lizundia E, Kundu D. Advances in natural biopolymer-based electrolytes and separators for battery applications. *Adv Funct Mater*. 2021;31(3):2005646. doi:10.1002/adfm.202005646.
11. Yang W, Yang W, Zeng J, Chen Y, Huang Y, Liu J, et al. Biopolymer-based gel electrolytes for electrochemical energy storage: advances and prospects. *Prog Mater Sci*. 2024;144:101264. doi:10.1016/j.pmatsci.2024.101264.
12. Zhang J, Huang X, Fu J, Huang Y, Liu W, Tang X. Novel PEO-based composite solid polymer electrolytes incorporated with active inorganic-organic hybrid polyphosphazene microspheres. *Mat Chem Phys*. 2010;121(3):511–8. doi:10.1016/j.matchemphys.2010.02.016.
13. Blesstina SRK, Mathavan T, Buvaneshwari P, Joel T, Benial AMF. Conducting behaviour of a novel solid biopolymer electrolyte for electrochemical application. *Ionics*. 2023;29(9):3437–50. doi:10.1007/s11581-023-05087-8.

14. Murmu R, Roy D, Sutar H, Senapati P, Abhisek Mohapatra S. Effect of sulfuric acid on the physiochemical properties of chitosan-PVA blend for direct methanol fuel cell. *J Polym Mater.* 2022;39(1–2):89–109. doi:10.32381/JPM.2022.39.1-2.6.
15. Wang Q-J, Zhang P, Wang B, Fan L-Z. A novel gel polymer electrolyte based on trimethylolpropane trimethylacrylate/ionic liquid via *in situ* thermal polymerization for lithium-ion batteries. *Electrochim Acta.* 2021;370:137706. doi:10.1016/j.electacta.2020.137706.
16. Saadiah MA, Zhang D, Nagao Y, Muzakir SK, Samsudin AS. Reducing crystallinity on thin film based CMC/PVA hybrid polymer for application as a host in polymer electrolytes. *J Non-Crystall Solids.* 2019;511:201–11. doi:10.1016/j.jnoncrysol.2018.11.032.
17. Hadi JM, Aziz SB, Nofal MM, Hussien SA, Hamsan MH, Brza MA, et al. Electrical, dielectric property and electrochemical performances of plasticized silver ion-conducting chitosan-based polymer nanocomposites. *Membranes.* 2020;10(7):151. doi:10.3390/membranes10070151.
18. Li L, Shan Y, Yang X. New insights for constructing solid polymer electrolytes with ideal lithium-ion transfer channels by using inorganic filler. *Mater Today Commun.* 2021;26(5):101910. doi:10.1016/j.mtcomm.2020.101910.
19. Yazie N, Worku D, Gabbiye N, Alemayehu A, Getahun Z, Dagnew M. Development of polymer blend electrolytes for battery systems: recent progress, challenges, and future outlook. *Mat Renew Sustain Energy.* 2023;12(2):73–94. doi:10.1007/s40243-023-00231-w.
20. El-Sayed S, Mahmoud KH, Fatah AA, Hassen ADSC. TGA and dielectric properties of carboxymethyl cellulose/polyvinyl alcohol blends. *Phys B: Condens Matter.* 2011;406(21):4068–76. doi:10.1016/j.physb.2011.07.050.
21. Shukur MF, Kadir MFZ. Hydrogen ion conducting starch-chitosan blend based electrolyte for application in electrochemical devices. *Electrochimica Acta.* 2015;158:152–65. doi:10.1016/j.electacta.2015.01.167.
22. Utracki LA, Wilkie CA. *Polymer blends handbook.* Dordrecht, The Netherland: Kluwer Academic Publishers; 2002.
23. Hasan MM, Islam MD, Rashid TU. Biopolymer-based electrolytes for dye-sensitized solar cells: a critical review. *Energ Fuels.* 2020;34(12):15634–71. doi:10.1021/acs.energyfuels.0c03396.
24. Lakshminarayana K, Narasimha Rao VVR. Pyroelectric behaviour of polyvinyl alcohol (PVA)-polyvinyl pyrrolidone (PVP) polymer blend films. *Mater Lett.* 1997;30:65–71.
25. Kota S, Anantha R, Govada VR, Dumpala P. Chitosan/PVA films and silver nanoparticle impregnated nanofibrous dressings for evaluation of their wound healing efficacy in Wistar Albino rat model. *J Polym Mat.* 2024;40(3–4):285–303.
26. Rajendran S, Sivakumar M, Subadevi R. Investigations on the effect of various plasticizers in PVA-PMMA solid polymer blend electrolytes. *Mater Lett.* 2004;58(5):641–9. doi:10.1016/S0167-577X(03)00585-8.
27. Vahini M, Muthuvinayagam M. AC impedance studies on proton conducting biopolymer electrolytes based on pectin. *Mater Lett.* 2018;218:197–200. doi:10.1016/j.matlet.2018.02.011.
28. Ghazali NM, Mazuki NF, Samsudin AS. Characterization of biopolymer Blend-based on alginate and Poly(vinyl Alcohol) as an application for polymer host in polymer electrolyte. *Mat Today: Proc.* 2022;48:849–53.
29. Hema M, Selvasekarapandian S, Arunkumar D, Sakunthala A, Nithya HFTIR. XRD and ac impedance spectroscopic study on PVA based polymer electrolyte doped with NH_4X (X=Cl, Br, I). *J Non-Crystall Solids.* 2009;355(2):84–90. doi:10.1016/j.jnoncrysol.2008.10.009.
30. Buraidah MH, Arof AK. Characterization of chitosan/PVA blended electrolyte doped with NH_4I . *J Non-Cryst Solids.* 2011;357(16–17):3261–6.
31. Mishra R, Baskaran N, Ramakrishnan PA, Rao KJ. Lithium ion conduction in extreme polymer in salt regime. *Sol State Ion.* 1998;112(3):261–73.
32. Pawlicka A, Tavares FC, Dörr DS, Cholant CM, Ely F, Santos MJL, et al. Dielectric behavior and FTIR studies of xanthan gum-based solid polymer electrolytes. *Electrochim Acta.* 2019;305:232–9. doi:10.1016/j.electacta.2019.03.055.
33. Moniha V, Alagar M, Selvasekarapandian S, Sundaresan B, Boopathi G. Conductive bio-polymer electrolyte iota-carrageenan with ammonium nitrate for application in electrochemical devices. *J Non-Crystall Solids.* 2018;481:424–34. doi:10.1016/j.jnoncrysol.2017.11.027.

34. Nidhi, Patel S, Kumar R. Synthesis and characterization of magnesium ion conductivity in PVDF based nanocomposite polymer electrolytes disperse with MgO. *J Alloy Compoun.* 2019;789:6–14. doi:10.1016/j.jallcom.2019.03.089.
35. Hema M, Selvasekerapandian S, Sakunthala A, Arunkumar D, Nithya H. Structural, vibrational and electrical characterization of PVA-NH₄Br polymer electrolyte system. *Phys B: Condens Matter.* 2008;403(17):2740–7. doi:10.1016/j.physb.2008.02.001.
36. Mazuki NF, Fuzlin AF, Saadiah MA, Samsudin AS. An investigation on the abnormal trend of the conductivity properties of CMC/PVA-doped NH₄Cl-based solid biopolymer electrolyte system. *Ionics.* 2018;25(6):2657–67.
37. Anantha PS, Hariharan K. AC Conductivity analysis and dielectric relaxation behaviour of NaNO₃-Al₂O₃ composites. *Mat Sci Eng: B.* 2005;121(1–2):12–9.
38. Mohamad Isa MIN, Ramli M. Conductivity study of Carboxyl methyl cellulose Solid biopolymer electrolytes (SBE) doped with Ammonium Fluoride. *Earth Sci Res J.* 2014;3:59–66.
39. Fuzlin AF, Rasali NMJ, Samsudin AS. Effect on Ammonium Bromide in dielectric behavior based Alginate Solid Biopolymer electrolytes. *IOP Conf Ser: Mat Sci Eng.* 2018;342(1):012080.
40. Noor NAM, Isa MIN. Ionic conductivity and dielectric properties of CMC doped NH₄SCN solid biopolymer electrolytes. *Adv Mat Res.* 2015;1107:230–5.
41. Isa MIN, Samsudin AS. An enhancement on electrical properties of carboxymethyl cellulose-NH₄Br based biopolymer electrolytes through impedance characterization. *Int J Polym Anal Character.* 2017;22(5):447–54. doi:10.1080/1023666X.2017.1316630.
42. Kamarudin KH, Mohamad Isa MIN. Ionic conductivity via quantum mechanical tunneling in NH₄NO₃ doped carboxymethyl cellulose solid biopolymer electrolytes. *Adv Mat Res.* 2015;1107:236–41.
43. Bakar NYA, Muhamaruesa NHM, Aniskari NAB, Isa MINM. Electrical studies of carboxy methylcellulose-chitosan blend biopolymer doped Dodecyltrimethyl ammonium bromide solid electrolytes. *American J Appl Sci.* 2015;12(1):40–6. doi:10.3844/ajassp.2015.40.46.
44. Fuzlin AF, Sahraoui B, Samsudin AS. Influence of lithium bromide on electrical properties in bio-based polymer electrolytes. *Makara J Technol.* 2020;24(3):106–10. doi:10.7454/mst.v24i3.
45. Woo HJ, Majid SR, Arof AK. Dielectric properties and morphology of polymer electrolyte based on poly(ϵ -caprolactone) and ammonium thiocyanate. *Mater Chem Phys.* 2012;134(2–3):755–61.
46. Aziz SB, Abdullah RM, Rasheed MA, Ahmed HM. Role of ion dissociation on DC conductivity and silver nanoparticle formation in PVA: AgNt based polymer electrolytes: deep insights to ion transport mechanism. *Polymers.* 2017;9(8):338. doi:10.3390/polym9080338.
47. Buraidah MH, Teo LP, Arof AK. Conductivity studies of chitosan based solid polymer electrolyte incorporated with ionic liquid. In: *National Workshop on Functional Materials 2009*; 2009 Jun 16; Kuala Lumpur, Malaysia.
48. Lago J, Battle PD, Rosseinsky MJ, Coldea AI, Singleton J. Non-adiabatic small polaron hopping in the $n = 3$ Ruddlesden-Popper compound Ca₄Mn₃O₁₀. *J Phy: Condens Matter.* 2003;15(40):6817.